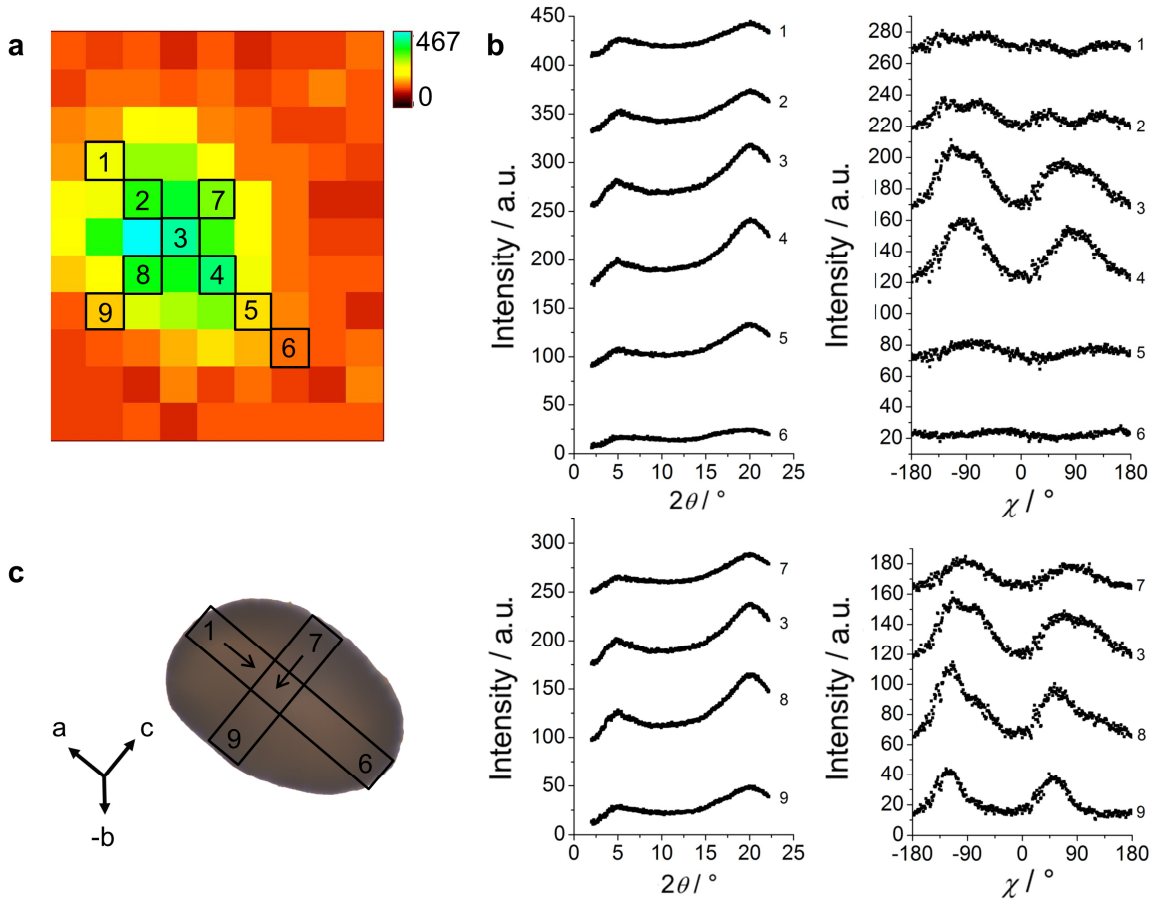

Supplementary Figure S1 | Detailed representation of the WAXS data of the LCE core-shell particle in Figure 4. a, X-ray absorption scan to localize the core-shell particle on the substrate. The particle was placed on a low-scattering adhesive stripe attached to the sample holder. Measurements were conducted along the axis *a* and *c* of the particle. **b**, Diffraction patterns I(2θ) and their corresponding azimuthal intensity distribution I(χ) for all measured positions: $\chi = 0°$ was shifted to compensate the tilted position of 60° of the core-shell particle with respect to the X-ray beam as seen in the nanography. The diffraction patterns I(2θ) show two broad halos as expected for nematics. A detailed explanation for the observed azimuthal intensity distributions I(χ) is given in the main text. **c**, Light microscope photo of the particle with a graphical representation of the particle regions sampled by the X-ray beam.

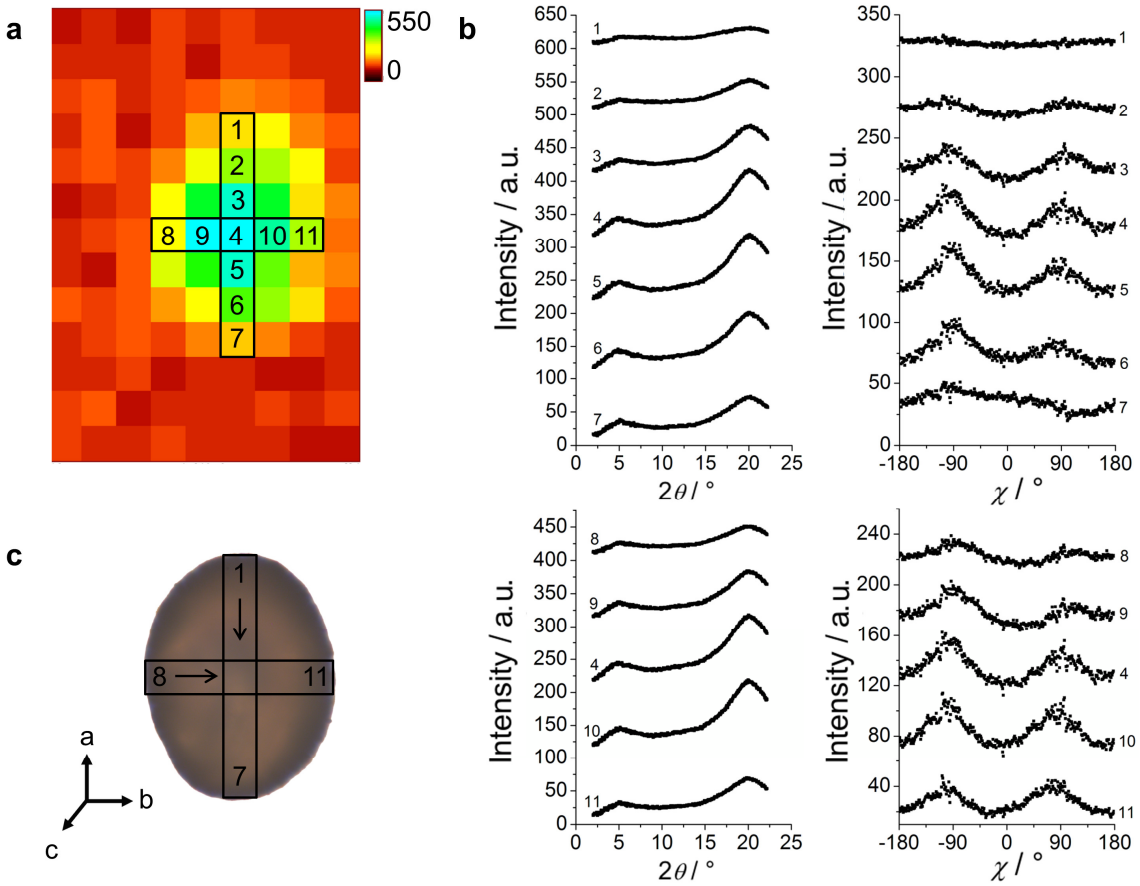

Supplementary Figure S2 | WAXS data of a second LCE core-shell particle flipped on its oblate side. a, X-ray absorption scan. Measurements were conducted along the axis *a* and *b* of the particle. **b,** Diffraction patterns I(2θ) and azimuthal intensity distributions I(χ). With two maxima at χ = -90° and +90° the radial intensity distributions I(χ) of the wide-angle halo indicate a director orientation along the long axis *a* of the particle. At positions 1 and 7, the top and bottom of axis *a*, the maxima deviate caused by the locally changing director field n at the poles of the particle. **c**, Position of the particle on the substrate with respect to the X-ray beam, as observed with light microscopy.

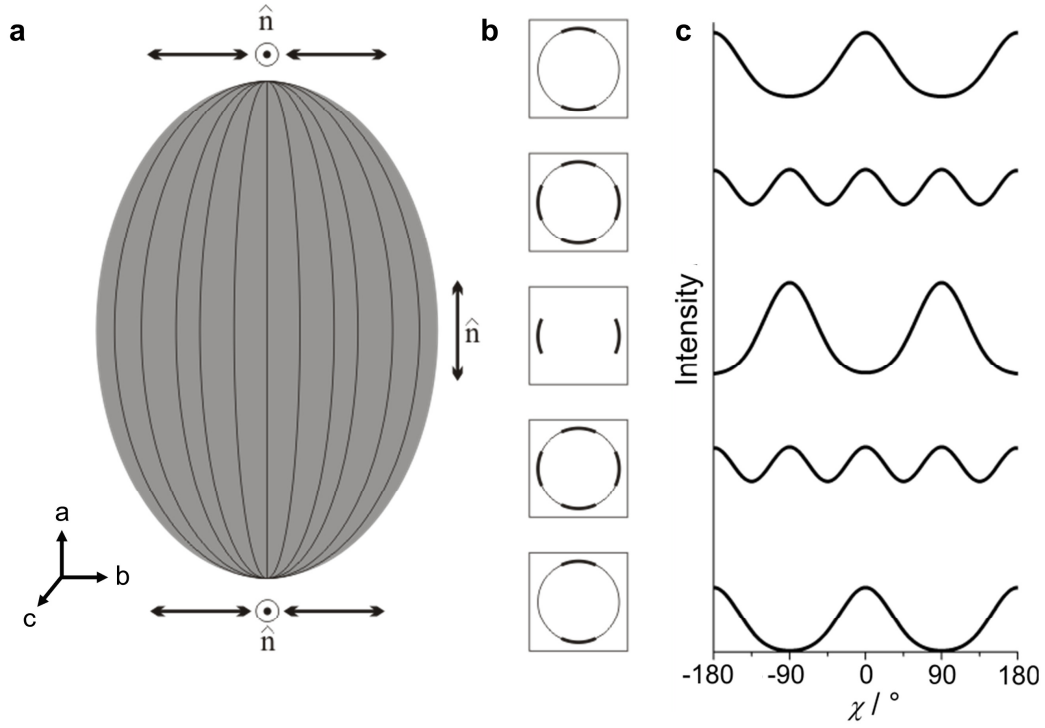

Supplementary Figure S3 | Influence of the director configuration on the azimuthal intensity distribution I(χ). a, Schematic drawing of the bipolar director alignment within the shell. **b**, Two-dimensional X-ray patterns measured at different positions along the axis *a* in the particle. **c**, Integration of the X-ray pattern in dependence of the azimuthal angle χ. At the top and the bottom of the particle the director is aligned perpendicular to the axis *a* which leads to two maxima in the integrated X-ray intensity I(χ) at $\chi = 0°$ and 180°. In the middle of the particle the director $\hat{n}$ aligns parallel to the axis *a*. The intensity profile shows here also two maxima which are now located at the angles $\chi = 90$ and -90°. If the X-ray measurements are performed close to the top or the bottom of the particle both orientations of the director can be observed. In this case, the intensity profile I(χ) shows four distinct maxima.

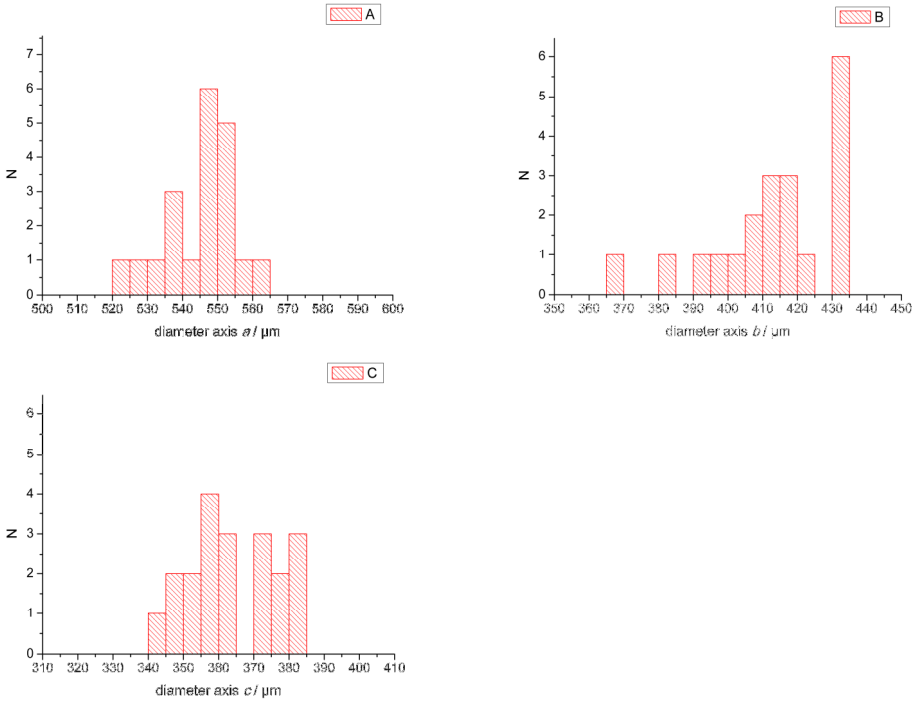

Supplementary Figure S4 | Bar plots of the particle size dispersity. 20 Particles were measured in total, giving the following results: axis A: 545 μm (±10 μm, 2%); axis B: 413 μm (±18 μm, 4%); axis C: 364 μm (±12 μm, 3%).

Supplementary Table S1 | Temperature dependence of glycerol viscosity. The viscosity values of glycerol in the temperature range relevant for this study decrease as follows.

T (°C)	viscosity (P)
37.0	3.8
42.0	2.7
48.0	1.8
60.0	0.9
65.0	0.7
73.0	0.5
83.0	0.4
90.0	0.3
130.0	0.3